



Title	Non-data-aided ML symbol timing estimation in MIMO correlated fading channels
Author(s)	Wu, YC; Serpedin, E
Citation	The 62nd IEEE Vehicular Technology Conference (VTC-2005-Fall), Dallas, TX., 25-28 September 2005. In Conference Proceedings, 2005, v. 4, p. 2091-2095
Issued Date	2005
URL	http://hdl.handle.net/10722/45944
Rights	©2005 IEEE. Personal use of this material is permitted. However, permission to reprint/republish this material for advertising or promotional purposes or for creating new collective works for resale or redistribution to servers or lists, or to reuse any copyrighted component of this work in other works must be obtained from the IEEE.

Non-data-aided ML Symbol Timing Estimation in MIMO Correlated Fading Channels

Yik-Chung Wu and Erchin Serpedin

Department of Electrical Engineering, Texas A&M University, College Station, TX 77843-3128, USA.

Email: {ycwu, serpedin}@ee.tamu.edu

Abstract—In this paper, the non-data-aided (NDA) maximum likelihood (ML) symbol timing estimator in MIMO correlated channel is derived. It is found that the extended square nonlinearity estimator in [9] is just a special case of the proposed algorithm. Furthermore, the conditional Cramer-Rao bound (CCRB) and the modified Cramer-Rao bound (MCRB) are also established. Simulation results under different operating conditions (e.g., number of antennas and correlation between antennas) are given to assess the performances of the NDA ML estimator and it is found that the mean square errors (MSE)s of the NDA ML estimator i) are close to the CCRBs, but not the MCRBs; ii) are approximately independent of the number of transmit antennas; iii) are inversely proportional to the number of receive antennas and iv) correlation between antennas has little effect on the MSE performance.

I. INTRODUCTION

Communication over Multiple-input multiple-output (MIMO) channel has attracted much attention recently due to the huge capacity gain over single antenna system. While many different techniques and algorithms have been proposed to explore the potential capacity, synchronization in MIMO channel received relatively less attention.

Symbol timing synchronization in MIMO uncorrelated flat fading channel was first studied by Naguib *et al.* [4], where orthogonal training sequences are employed. This algorithm was extended by the authors in [8] to increase its estimation accuracy. Recently, the true maximum likelihood symbol timing estimator based on training sequences was derived in [12]. While all the above mentioned symbol timing synchronization algorithms are data-aided, there is not much discussion on non-data-aided (NDA) estimators. The only one reported in the literature is [9], where the well-known square nonlinearity estimator [10] in single antenna system was extended to MIMO channel.

In this paper, the NDA ML symbol timing estimator in MIMO channel is derived. Particularly, we consider correlated fading between antennas. It is found that the extended square nonlinearity estimator in [9] is just a special case of the proposed algorithm. Furthermore, the conditional Cramer-Rao bound (CCRB) and modified Cramer-Rao bound (MCRB) are also derived for comparison. Simulation results under different operating conditions (e.g., number of antennas and correlation between antennas) are given to assess the performances of the NDA ML estimator and it is found that i) the MSEs of the NDA ML estimator are close to the corresponding CCRBs, but not MCRBs; ii) the MSEs are approximately

independent of the number of transmit antennas; iii) the MSEs are inversely proportional to the number of receive antennas and iv) correlation between antennas has little effect on the MSE performance.

II. SIGNAL MODEL

Consider a MIMO communication system with N transmit and M receive antennas. At each receiving antenna, a superposition of faded signals from all the transmit antennas plus noise is received. The complex envelope of the received signal at the j^{th} receive antenna can be written as

$$r_j(t) = \sqrt{\frac{E_s}{NT}} \sum_{i=1}^N h_{ij} \sum_n d_i(n) g(t - nT - \varepsilon_o T) + \eta_j(t),$$

$$j = 1, 2, \dots, M$$
(1)

where E_s/N is the symbol energy; h_{ij} 's are the complex channel coefficients between the i^{th} transmit antenna and the j^{th} receive antenna; $d_i(n)$ is the zero-mean complex valued symbol transmitted from the i^{th} transmit antenna; $g(t)$ is the transmit filter with unit energy; T is the symbol duration; $\varepsilon_o \in [0, 1)$ is the uniformly distributed unknown timing offset and $\eta_j(t)$ is the complex-valued circularly distributed Gaussian white noise at the j^{th} receive antenna, with power density N_o . Throughout this paper, it is assumed that the channel is frequency flat and quasi-static.

After passing through the anti-aliasing filter, the received signal is then sampled at rate $f_s = 1/T_s$, where $T_s \triangleq T/Q$. Note that the oversampling factor Q is determined by the frequency span of $g(t)$; if $g(t)$ is bandlimited to $f = \pm 1/T$ (an example of which is the root raised cosine pulse), $Q = 2$ is sufficient. The received vector \mathbf{r}_j , which consists of $L_o Q$ consecutive received samples (L_o is the observation length), can be expressed as (without loss of generality, we consider the received sequence start at $t = 0$)

$$\mathbf{r}_j = \xi \mathbf{A}_{\varepsilon_o} \mathbf{Z} \mathbf{H}_{j,:}^T + \boldsymbol{\eta}_j,$$
(2)

where¹ $\xi \triangleq \sqrt{E_s/NT}$,

$$\mathbf{r}_j \triangleq [r_j(0) \ r_j(T_s) \ \dots \ r_j((L_o Q - 1)T_s)]^T,$$
(3)

$$\mathbf{A}_{\varepsilon} \triangleq [\mathbf{a}_{-L_g}(\varepsilon) \ \mathbf{a}_{-L_g+1}(\varepsilon) \ \dots \ \mathbf{a}_{L_o+L_g-1}(\varepsilon)],$$
(4)

¹Notation \mathbf{x}^T denotes the transpose of \mathbf{x} , and \mathbf{x}^H denotes the transpose conjugate of \mathbf{x} .

$$\mathbf{a}_i(\varepsilon) \triangleq [g(-iT - \varepsilon T) g(T_s - iT - \varepsilon T) \dots g((L_o Q - 1)T_s - iT - \varepsilon T)]^T, \quad (5)$$

$$\mathbf{Z} \triangleq [\mathbf{d}_1 \mathbf{d}_2 \dots \mathbf{d}_N], \quad (6)$$

$$\mathbf{d}_i \triangleq [d_i(-L_g) d_i(-L_g + 1) \dots d_i(L_o + L_g - 1)]^T \quad (7)$$

$$\boldsymbol{\eta}_j \triangleq [\eta_j(0) \eta_j(1) \dots \eta_j(L_o Q - 1)]^T, \quad (8)$$

$$\mathbf{H} \triangleq \begin{bmatrix} h_{11} & h_{21} & \dots & h_{N1} \\ h_{12} & h_{22} & \dots & h_{N2} \\ \vdots & & & \vdots \\ h_{1M} & h_{2M} & \dots & h_{NM} \end{bmatrix}, \quad (9)$$

with $\mathbf{H}_{j\cdot}$ denotes the j^{th} row of matrix \mathbf{H} , $\eta(i) \triangleq \eta(iT/Q)$, and L_g denotes the number of symbols affected by the inter-symbol interference (ISI) introduced by one side of $g(t)$.

Stacking the received vectors from all the M received antennas gives²

$$\mathbf{r} = \xi(\mathbf{I}_M \otimes \mathbf{A}_{\varepsilon_o}) \text{vec}(\mathbf{Z}\mathbf{H}^T) + \boldsymbol{\eta} \quad (10)$$

where $\mathbf{r} \triangleq [\mathbf{r}_1^T \mathbf{r}_2^T \dots \mathbf{r}_M^T]^T$, $\boldsymbol{\eta} \triangleq [\boldsymbol{\eta}_1^T \boldsymbol{\eta}_2^T \dots \boldsymbol{\eta}_M^T]^T$ and \mathbf{I}_M is the $M \times M$ identity matrix.

In order to include the correlation between channel coefficients, we write

$$\mathbf{H} = \sqrt{\boldsymbol{\Phi}_R} \mathbf{H}_{\text{i.i.d.}} \sqrt{\boldsymbol{\Phi}_T}^T \quad (11)$$

where $\boldsymbol{\Phi}_T$ and $\boldsymbol{\Phi}_R$ are the power correlation matrices [7] of transmit antennas and receive antennas arrays (which is assumed known), respectively; $\mathbf{H}_{\text{i.i.d.}} \in \mathbb{C}^{M \times N}$ containing independently and identically distributed (i.i.d.) zero-mean, unit-variance, circularly symmetric complex Gaussian entries and the square roots are the matrix square root (i.e., Cholesky factorization) such that $\sqrt{\boldsymbol{\Phi}} \sqrt{\boldsymbol{\Phi}}^H = \boldsymbol{\Phi}$. Note that (11) models the correlation among transmit and receive antennas array independently. This model is based on the assumption that only immediate surroundings of the antenna array impose the correlation between antennas array elements and have no impact on the correlation at the other end of the communication link. The validity of this model is verified by recent measurements [5]-[7]. Putting (11) into (10), we have

$$\mathbf{r} = \xi(\mathbf{I}_M \otimes \mathbf{A}_{\varepsilon_o}) \text{vec}(\mathbf{Z} \sqrt{\boldsymbol{\Phi}_T} \mathbf{H}_{\text{i.i.d.}}^T \sqrt{\boldsymbol{\Phi}_R}^T) + \boldsymbol{\eta}. \quad (12)$$

III. NON-DATA-AIDED ML ESTIMATOR

In this case, no training sequence is used and \mathbf{Z} contains real data. Now, the matrices \mathbf{Z} and $\mathbf{H}_{\text{i.i.d.}}$ in (12) are unknown. Using the identity $\text{vec}(\mathbf{A}\mathbf{Y}\mathbf{B}) = (\mathbf{B}^T \otimes \mathbf{A}) \text{vec}(\mathbf{Y})$, (12) can be rewritten in the following form

$$\begin{aligned} \mathbf{r} &= \xi(\mathbf{I}_M \otimes \mathbf{A}_{\varepsilon_o}) (\sqrt{\boldsymbol{\Phi}_R} \otimes \mathbf{I}_{L_o + 2L_g}) \text{vec}(\mathbf{Z} \sqrt{\boldsymbol{\Phi}_T} \mathbf{H}_{\text{i.i.d.}}^T) + \boldsymbol{\eta} \\ &= \xi(\sqrt{\boldsymbol{\Phi}_R} \otimes \mathbf{A}_{\varepsilon_o}) \text{vec}(\mathbf{Z} \sqrt{\boldsymbol{\Phi}_T} \mathbf{H}_{\text{i.i.d.}}^T) + \boldsymbol{\eta}, \end{aligned} \quad (13)$$

where the last line come from the fact that $(\mathbf{A} \otimes \mathbf{B})(\mathbf{C} \otimes \mathbf{D}) = (\mathbf{A}\mathbf{C}) \otimes (\mathbf{B}\mathbf{D})$. Note that although $\boldsymbol{\Phi}_T$ is assumed to be known, it cannot be separated from \mathbf{Z} and $\mathbf{H}_{\text{i.i.d.}}$ because

²Notation \otimes denotes Kronecker products and $\text{vec}(\mathbf{H})$ denotes a $MN \times 1$ vector formed by stacking the columns of \mathbf{H} under each other.

the correlation in transmit antennas can be translated into correlation of unknown data or vice versa.

Since the noise is white and Gaussian, the joint ML estimate of ε_o and $\text{vec}(\mathbf{Z} \sqrt{\boldsymbol{\Phi}_T} \mathbf{H}_{\text{i.i.d.}}^T)$ is given by maximizing

$$p(\mathbf{r}|\varepsilon, \mathbf{x}) = \frac{1}{(\pi N_o)^{L_o Q}} \exp \left[-\frac{(\mathbf{r} - \check{\mathbf{A}}_\varepsilon \mathbf{x})^H (\mathbf{r} - \check{\mathbf{A}}_\varepsilon \mathbf{x})}{N_o} \right], \quad (14)$$

or equivalently minimizing

$$J(\mathbf{r}|\varepsilon, \mathbf{x}) = (\mathbf{r} - \check{\mathbf{A}}_\varepsilon \mathbf{x})^H (\mathbf{r} - \check{\mathbf{A}}_\varepsilon \mathbf{x}), \quad (15)$$

where $\check{\mathbf{A}}_\varepsilon \triangleq \xi(\sqrt{\boldsymbol{\Phi}_R} \otimes \mathbf{A}_\varepsilon)$, ε and \mathbf{x} are the trial values for ε_o and $\text{vec}(\mathbf{Z} \sqrt{\boldsymbol{\Phi}_T} \mathbf{H}_{\text{i.i.d.}}^T)$, respectively.

With the linear model of (13), the ML estimate for $\text{vec}(\mathbf{Z} \sqrt{\boldsymbol{\Phi}_T} \mathbf{H}_{\text{i.i.d.}}^T)$ (as a function of ε) is given by [14]

$$\hat{\mathbf{x}} = (\check{\mathbf{A}}_\varepsilon^H \check{\mathbf{A}}_\varepsilon)^{-1} \check{\mathbf{A}}_\varepsilon^H \mathbf{r}. \quad (16)$$

Putting (16) into (15), after some straightforward calculations and dropping the irrelevant terms, the ML symbol timing estimator reduces to the maximization of the following likelihood function:

$$\Lambda(\varepsilon) = \mathbf{r}^H \check{\mathbf{A}}_\varepsilon (\check{\mathbf{A}}_\varepsilon^H \check{\mathbf{A}}_\varepsilon)^{-1} \check{\mathbf{A}}_\varepsilon^H \mathbf{r}. \quad (17)$$

It can be easily shown that

$$\check{\mathbf{A}}_\varepsilon (\check{\mathbf{A}}_\varepsilon^H \check{\mathbf{A}}_\varepsilon)^{-1} \check{\mathbf{A}}_\varepsilon^H = \mathbf{I}_M \otimes \mathbf{A}_\varepsilon (\mathbf{A}_\varepsilon^H \mathbf{A}_\varepsilon)^{-1} \mathbf{A}_\varepsilon^H, \quad (18)$$

which gives

$$\Lambda(\varepsilon) = \sum_{j=1}^M \mathbf{r}_j^H \mathbf{A}_\varepsilon (\mathbf{A}_\varepsilon^H \mathbf{A}_\varepsilon)^{-1} \mathbf{A}_\varepsilon^H \mathbf{r}_j. \quad (19)$$

The NDA ML symbol timing estimation can be stated as

$$\hat{\varepsilon} = \arg \max_{\varepsilon} \Lambda(\varepsilon). \quad (20)$$

We make the following remarks:

- 1) The correlations in the transmit and receive antenna arrays do not appear in the estimator. That is, the NDA ML symbol timing estimator is independent of the antennas correlation.
- 2) The likelihood function at each receive antenna can be calculated independently and then added together to obtain the overall likelihood function. Furthermore, for each of the receive antenna, the likelihood function is the same as the likelihood function for single antenna systems [11], [16].
- 3) In single antenna systems, a low-complexity technique was proposed in [11] to maximize the likelihood function for symbol timing estimation. It was further shown that the resultant estimator reduces to the well-known square nonlinearity estimator [10] under certain conditions. In the present MIMO case, the low-complexity maximization technique [11] can also be applied to the proposed estimator (20). With the same arguments and conditions in [11], it can be easily shown that the proposed estimator (20) reduces to the extended square nonlinearity estimator in [9].

4) Notice that although the low-complexity maximization technique in [11] can be applied to the proposed estimator (20) and this results in an estimator with pretty good performance, however, the low-complexity maximization technique involves an approximation, which causes incomplete cancelation of self-noise at high SNRs. Therefore, we do not pursue this direction in this paper. Instead, a two-step maximization approach is employed. The first step (coarse search) computes $\Lambda(\varepsilon)$ over a grid of timing delay $\varepsilon_k \triangleq k/K$ for $k = 0, 1, \dots, K-1$, and then the ε_k that maximizes $\Lambda(\varepsilon)$ is selected. The second step (fine search) finds the global maximum by using either gradient method [17], dichotomous search [15], or interpolation [15]. In this paper, we employ the parabolic interpolation in the second step due to its implementation simplicity. More specifically, assume that $\Lambda(\varepsilon_{\hat{k}})$ is identified as the maximum among all $\Lambda(\varepsilon_k)$ in the first step. Define $I_1 \triangleq \Lambda(\varepsilon_{\hat{k}-1})$, $I_2 \triangleq \Lambda(\varepsilon_{\hat{k}})$ and $I_3 \triangleq \Lambda(\varepsilon_{\hat{k}+1})$, then [15]

$$\hat{\varepsilon} = \varepsilon_{\hat{k}} + \frac{I_1 - I_3}{2K(I_1 + I_3 - 2I_2)}. \quad (21)$$

IV. PERFORMANCE BOUNDS

In this section, we presented two performance bounds, namely conditional Cramer-Rao bound (CCRB) and modified Cramer-Rao bound (MCRB). CCRB is the Cramer-Rao bound conditioned that the nuisance parameters are treated as deterministic and are jointly estimated together with the unknown parameter of interest (symbol timing). Therefore, the CCRB serves as a performance lower bound for the NDA ML estimator derived. On the other hand, the MCRB is a lower bound for *any* unbiased symbol timing estimator, irrespective of the underlying assumption about the nuisance parameters and it serves as the ultimate estimation accuracy that may be achieved. Due to space limitation, only the results are presented. The detailed derivation can be found in [13]. It can be shown that the CCRB for symbol timing estimation in MIMO correlated fading channel (for a specific ε_o) is given by³ [13]

$$\text{CCRB}(\varepsilon_o) = \frac{1}{2M \text{tr}(\tilde{\mathbf{D}}_{\varepsilon_o}^H \mathbf{P}_{\mathbf{A}}^\perp \tilde{\mathbf{D}}_{\varepsilon_o} \boldsymbol{\Psi}/N)} \left(\frac{E_s}{N_o}\right)^{-1}. \quad (22)$$

where

$$\tilde{\mathbf{D}}_\varepsilon \triangleq \frac{1}{\sqrt{Q}} \frac{d\mathbf{A}_\varepsilon}{d\varepsilon}, \quad (23)$$

$$\mathbf{P}_{\mathbf{A}}^\perp \triangleq \mathbf{I}_{L_o Q} - \mathbf{A}_{\varepsilon_o} (\mathbf{A}_{\varepsilon_o}^H \mathbf{A}_{\varepsilon_o})^{-1} \mathbf{A}_{\varepsilon_o}^H, \quad (24)$$

and $\boldsymbol{\Psi}$ is a Hermitian and Toeplitz matrix with elements $[\boldsymbol{\Psi}]_{ij} \triangleq \text{tr}(\boldsymbol{\Gamma}_z(j-i) \boldsymbol{\Phi}_T)$ and $\boldsymbol{\Gamma}_z(j-i) \triangleq \mathbb{E}[(\mathbf{Z}^*)_{j,:}^T (\mathbf{Z})_{i,:}]$ is the average cross-correlation matrix of the symbols transmitted with time index difference $j-i$.

³Strictly speaking, the bound given is the asymptotic CCRB. However, it is shown in [16] that the true CCRB tends to the asymptotic CCRB when $M, N \rightarrow \infty$

For the MCRB, it can be shown that it is given by [13]

$$\text{MCRB}(\varepsilon_o) = \frac{1}{2M \text{tr}(\tilde{\mathbf{D}}_{\varepsilon_o}^H \tilde{\mathbf{D}}_{\varepsilon_o} \boldsymbol{\Psi}/N)} \left(\frac{E_s}{N_o}\right)^{-1}. \quad (25)$$

Since ε_o is assumed to be uniformly distributed within $[0, 1)$, the average of CCRB and MCRB can be computed by numerical integration of (22) and (25), respectively. In the following, we consider two special cases.

Special Case 1: The data is spatially and temporally white (e.g., Vertical-Bell Labs Layered Space-Time (V-BLAST) system⁴ [1]). In this case, $\boldsymbol{\Gamma}_z(j-i) = \mathbf{I}_N \delta_{ij}$, implying that $[\boldsymbol{\Psi}]_{ij} = \delta_{ij} \text{tr}(\boldsymbol{\Phi}_T) = N \delta_{ij}$. Therefore, the corresponding CCRB and MCRB are

$$\text{CCRB}(\varepsilon_o) = \frac{1}{2M \text{tr}(\tilde{\mathbf{D}}_{\varepsilon_o}^H \mathbf{P}_{\mathbf{A}}^\perp \tilde{\mathbf{D}}_{\varepsilon_o})} \left(\frac{E_s}{N_o}\right)^{-1} \quad (26)$$

and

$$\text{MCRB}(\varepsilon_o) = \frac{1}{2M \text{tr}(\tilde{\mathbf{D}}_{\varepsilon_o}^H \tilde{\mathbf{D}}_{\varepsilon_o})} \left(\frac{E_s}{N_o}\right)^{-1}, \quad (27)$$

respectively. Note that in this case, the CCRB and MCRB do not depend on the number of transmit antennas and the correlations among antennas.

Special Case 2: Space-Time Block Code (STBC) system. In general, a block of space-time block coded symbols can be represented by a $s \times N$ matrix [3]

$$\mathcal{G} = \sum_{k=1}^{rs} \Re(b_k) \mathbf{X}_k + \mathbf{j} \sum_{k=1}^{rs} \Im(b_k) \mathbf{Y}_k, \quad (28)$$

where r is the rate of the STBC, s is the length of the STBC, b_k 's are the i.i.d., complex valued symbols to be encoded, $\Re(\cdot)$ and $\Im(\cdot)$ denote the real and imaginary parts, $\mathbf{j} \triangleq \sqrt{-1}$ and $\mathbf{X}_k, \mathbf{Y}_k$ are the fixed, real-valued elementary code matrices. Without loss of generality, we assume $|b_k| = 1$. It is proved in [13] that for the STBC system,

$$\boldsymbol{\Gamma}_z(j-i) = \begin{cases} \mathbf{0}_N & \text{for } |j-i| \geq s \\ \frac{1}{2s} \sum_{n=1}^{s-\ell} \left(\sum_{k=1}^{rs} [\mathbf{X}_k]_{n+\ell,:}^T [\mathbf{X}_k]_{n,:} \right) & \text{for } |j-i| = \ell, \\ \sum_{k=1}^{rs} [\mathbf{Y}_k]_{n+\ell,:}^T [\mathbf{Y}_k]_{n,:} & \ell < s \end{cases} \quad (29)$$

For example, let us consider the half-rate orthogonal space-time block code with four transmit antennas [2], in which case $N = 4$, $s = 8$, $r = 1/2$ and the matrix \mathcal{G} given by

$$\mathcal{G} = \begin{pmatrix} b_1 & b_2 & b_3 & b_4 \\ -b_2 & b_1 & -b_4 & b_3 \\ -b_3 & b_4 & b_1 & -b_2 \\ -b_4 & -b_3 & b_2 & b_1 \\ b_1^* & b_2^* & b_3^* & b_4^* \\ -b_2^* & b_1^* & -b_4^* & b_3^* \\ -b_3^* & b_4^* & b_1^* & -b_2^* \\ -b_4^* & -b_3^* & b_2^* & b_1^* \end{pmatrix}. \quad (30)$$

⁴In its initial development, V-BLAST system does not employ any temporal error control code. Although temporal error control code may be applied in V-BLAST system, but at the same time, it is likely that interleaving would be used. So we assume the data is temporally white.

Decomposing \mathcal{G} in terms of \mathbf{X}_k and \mathbf{Y}_k and using (29), it is found that

$$\mathbf{\Gamma}_z(j-i) = \begin{cases} \mathbf{I}_4 & \text{for } i=j, \\ \frac{1}{4} \begin{bmatrix} 0 & 2 & 0 & 1 \\ -2 & 0 & 1 & 0 \\ 0 & -1 & 0 & 2 \\ -1 & 0 & -2 & 0 \end{bmatrix} & \text{for } |j-i|=1, \\ \frac{1}{4} \begin{bmatrix} 0 & 0 & 1 & 0 \\ 0 & 0 & 0 & 1 \\ 0 & -1 & 0 & 0 \\ -1 & 0 & 0 & 0 \end{bmatrix} & \text{for } |j-i|=3, \\ \mathbf{0}_4 & \text{otherwise.} \end{cases} \quad (31)$$

Then, $\mathbf{\Psi}$ can be computed according to $[\mathbf{\Psi}]_{ij} = \text{tr}(\mathbf{\Gamma}_z(j-i)\mathbf{\Phi}_T)$ and the CCRB and MCRB are given by (22) and (25), respectively.

V. SIMULATION RESULTS AND DISCUSSIONS

In this section, the MSE performance of the proposed symbol timing estimator is assessed by Monte Carlo simulations and then compared with the CCRB and MCRB presented in Section IV. In all the simulations, $L_o = 32$, $L_g = 4$, $Q = 2$, $K = 16$, ε_o is uniformly distributed in the range $[0, 1)$ and $g(t)$ being a root raised cosine filter with roll-off factor $\alpha = 0.3$. Each simulation point is obtained by averaging 10^4 simulation runs.

First, let assume $\mathbf{\Phi}_T = \mathbf{I}_N$, $\mathbf{\Phi}_R = \mathbf{I}_M$ and there is no space-time coding for the moment. The effect of correlation among antennas and space-time coding will be examined later. The effect of the number of transmit antennas N is shown Fig. 1 with $M = 4$. It can be seen that when the number of transmit antenna increases, the improvement in MSE is limited. Closer examination reveals that the CCRBs for different number of transmit antennas basically coincide. Therefore, the performance of the NDA ML estimator is approximately independent of N . Next, the effect of number of receive antennas M is shown in Fig. 2 with $N = 4$. It is clear that increasing M leads to considerable MSE improvements. Since from (22), the CCRB is inversely proportional to M and from Fig. 2, the performances of the proposed estimator are very close to their corresponding CCRBs, it can be concluded that the MSE of ML estimator is approximately inversely proportional to M .

Fig. 3 show the MSE performances of the proposed estimator for a 4×4 system under the effect of correlated fading among antennas and space-time coding. The measured correlation matrices from Nokia [7] are used in simulations:

$$\mathbf{\Phi}_T = \begin{bmatrix} 1 & 0.4154 & 0.2057 & 0.1997 \\ 0.4154 & 1 & 0.3336 & 0.3453 \\ 0.2057 & 0.3336 & 1 & 0.5226 \\ 0.1997 & 0.3453 & 0.5226 & 1 \end{bmatrix} \quad (32)$$

$$\mathbf{\Phi}_R = \begin{bmatrix} 1 & 0.3644 & 0.0685 & 0.3566 \\ 0.3644 & 1 & 0.3245 & 0.1848 \\ 0.0685 & 0.3245 & 1 & 0.3093 \\ 0.3566 & 0.1848 & 0.3093 & 1 \end{bmatrix}. \quad (33)$$

Three cases are considered in Fig. 3. The first one is no space-time coding and no fading correlation, which is shown using '+' markers. The second one is no space-time coding but with fading correlation, which is shown by 'o' markers.

The final one is that the data is encoded with the half rate space-time block code (30) and with correlated fading, which is shown by '.' markers. It can be seen that the presence of correlated fading and space-time coding do not affect the MSE performances of the proposed estimator. Furthermore, it can be seen that the MSEs of the proposed estimator are very close to the CCRBs. This means that proposed estimator is an efficient estimator conditioned that the nuisance parameters are being jointly estimated together with the unknown timing delay. Unfortunately, the CCRBs are quite far away from the MCRBs. Notice that, according to [16], CCRB is a valid bound only for estimators that rely on quadratic nonlinearity, there is a possibility that some other NDA estimators employing higher order (>2) nonlinearities would have performances closer to the MCRB. This is subject to further investigations.

VI. CONCLUSIONS

The non-data-aided ML symbol timing estimator in MIMO correlated channel has been derived and the corresponding CCRB and MCRB were also established. It was found that the extended square nonlinearity estimator in [9] is just a special case of the proposed algorithm. Simulation results were given to assess the performances of the proposed estimator and it was found that i) the MSEs of the proposed estimator are close to the CCRB but not MCRB; ii) the MSEs are approximately independent of the number of transmit antennas; iii) the MSEs are inversely proportional to the number of receive antennas and iv) correlation between antennas has little effect on the MSEs.

REFERENCES

- [1] G. J. Foschini, G. D. Golden, R. A. Valenzuela and P. W. Wolniansky, "Simplified processing for high spectral efficiency wireless communication employing multi-element arrays," *IEEE J. Select. Areas Commun.*, vol. 17, pp. 1841-1852, Nov. 1999.
- [2] V. Tarokh, H. Jafarkhani and A. R. Calderbank, "Space-time block coding for wireless communications: performance results," *IEEE J. Select. Areas in Commun.*, vol. 17, pp. 451-460, Mar. 1999.
- [3] E. G. Larsson, P. Stoica, and J. Li, "Orthogonal space-time block codes: maximum likelihood detection for unknown channels and unstructured interferences," *IEEE Trans. Signal Proc.*, vol. 51, pp. 362-372, Feb. 2003.
- [4] A. F. Naguib, V. Tarokh, N. Seshadri and A. R. Calderbank, "A space-time coding modem for high-data-rate wireless communications," *IEEE J. Select. Areas in Commun.*, vol. 16, pp. 1459-1478, Oct. 1998.
- [5] K. Yu, M. Bengtsson, B. Ottersten, D. McNamara, P. Karlsson and M. Beach, "Modeling of wide-band MIMO radio channels based on NLoS indoor measurements," *IEEE Trans. Veh. Tech.*, vol. 53, pp. 655-665, May. 2004.
- [6] D. Chizhik, J. Ling, P. W. Wolniansky, R. A. Valenzuela, N. Costa and K. Huber, "Multiple-input-multiple-output measurements and modeling in Manhattan," *IEEE J. Select. Areas in Commun.*, vol. 21, pp. 321-331, Apr. 2003.
- [7] L. Schumacher, J. P. Kermaol, F. Frederiksen, K. I. Pedersen, A. Algrans and P. E. Mogensen, "MIMO channel characterisation," *Deliverable D2 V1.1 of IST-1999-11729 METRA project*, pp. 1-57, Feb. 2001. Available online: <http://www.ist-metra.org>
- [8] Y.-C. Wu, S. C. Chan and E. Serpedin, "Symbol-timing estimation in space-time coding systems based on orthogonal training sequences," *IEEE Trans. on Wireless Communications*, vol. 4, no. 2, pp. 603-613, Mar. 2005.
- [9] Y.-C. Wu and S.-C. Chan, "On the symbol timing recovery in space-time coding systems," *Proceedings of IEEE Wireless Communications and Networking Conference (WCNC) 2003*, pp. 420-424, Mar. 2003.

- [10] M. Oerder and H. Meyr, "Digital filter and square timing recovery," *IEEE Trans. Commun.*, vol. 36, pp. 605-612, May 1988.
- [11] Y.-C. Wu and E. Serpedin, "Low-complexity feedforward symbol timing estimator using conditional maximum likelihood principle," *IEEE Commun. Letters*, vol. 8, pp. 168-170, May 2004.
- [12] Y.-C. Wu and E. Serpedin, "Data-aided maximum likelihood symbol timing estimation in MIMO correlated fading channels," *Proceedings of IEEE ICASSP 04*, vol. 4, pp. 829-832, May 2004.
- [13] Y.-C. Wu and E. Serpedin, "Symbol Timing Estimation in MIMO Correlated Flat-Fading Channels," *Wireless Communications and Mobile Computing*, Special Issue on MIMO Communications, Wiley, vol. 4, Issue 7, pp. 773-790, Nov. 2004.
- [14] S. M. Kay, *Fundamentals of Statistical Signal Processing - Estimation Theory*. Prentice Hall, 1993.
- [15] Y. V. Zakharov, V. M. Baronkin and T. C. Tozer, "DFT-based frequency estimators with narrow acquisition range," *IEE Proc.-Commun.*, Vol. 148, No. 1, pp. 1-7, Feb. 2001.
- [16] G. Vazquez and J. Riba, "Non-data-aided digital synchronization," in *Signal Processing Advanced in Wireless and Mobile Communications: Volume 2* (edited by G. B. Giannakis, Y. Hua, P. Stoica and L. Tong), Prentice Hall 2001.
- [17] B. Ottersten, M. Viberg, P. Stoica and A. Nehorai, "Exact and large sample maximum likelihood techniques for parameter estimation and detection in array processing," in *Radar array processing*, Springer-Verlag, 1993.

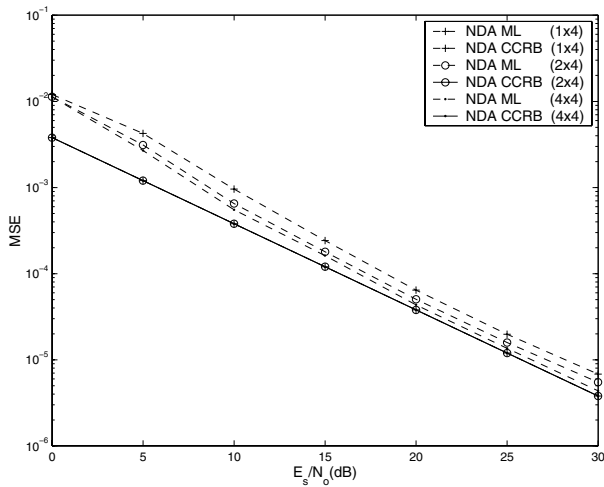


Fig. 1. MSEs of the proposed estimator with different number of transmit antennas (assuming $\Phi_T = \mathbf{I}_N$ and $\Phi_R = \mathbf{I}_M$).

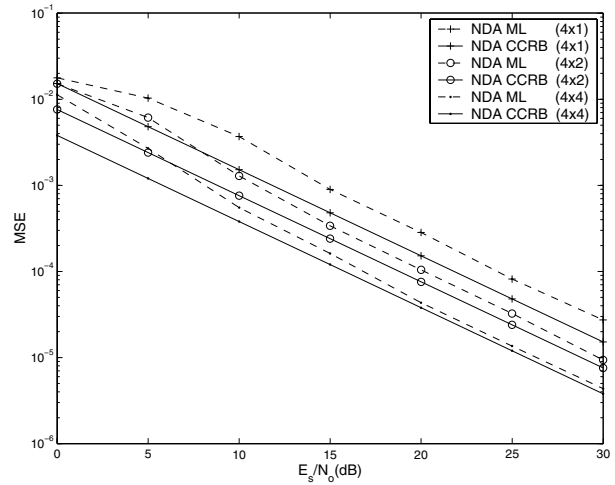


Fig. 2. MSEs of the proposed estimator with different number of receive antennas (assuming $\Phi_T = \mathbf{I}_N$ and $\Phi_R = \mathbf{I}_M$).

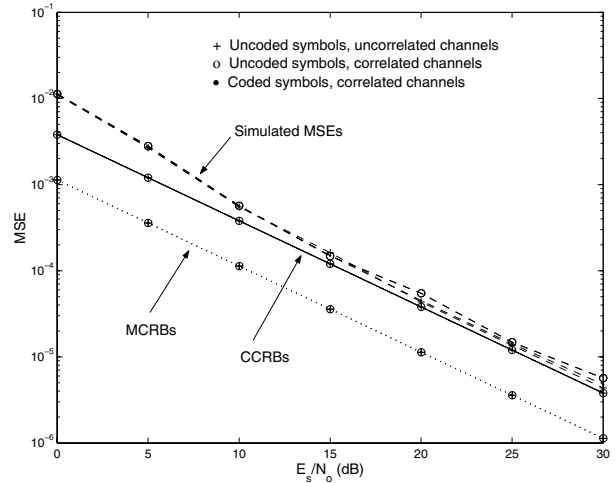


Fig. 3. MSEs of the proposed estimator under correlated fading between antennas and space-time coding for a 4×4 system.